

UNCLASSIFIED

AD NUMBER

AD816178

LIMITATION CHANGES

TO:

Approved for public release; distribution is unlimited.

FROM:

Distribution authorized to U.S. Gov't. agencies and their contractors;
Administrative/Operational Use; 30 JUN 1967.
Other requests shall be referred to Air Force Technical Applications Center, Washington, DC 20330.

AUTHORITY

AFTAC ltr 25 Jan 1972

THIS PAGE IS UNCLASSIFIED

AD816178

MULTIPLE COHERENCE OF SHORT PERIOD NOISE AT UBSO, AND TFSO

30 June 1967

Prepared For

AIR FORCE TECHNICAL APPLICATIONS CENTER

Washington, D. C.

By

E. F. Chiburis
W. C. Dean

TELEDYNE, INC.



Under

Project VELA UNIFORM

Sponsored By

ADVANCED RESEARCH PROJECTS AGENCY
Nuclear Test Detection Office
ARPA Order No. 624

MULTIPLE COHERENCE OF SHORT PERIOD NOISE AT UBSO AND TFSO

SEISMIC DATA LABORATORY REPORT NO.192

AFTAC Project No.:	VELA T/6702
Project Title:	Seismic Data Laboratory
ARPA Order No.:	624
ARPA Program Code No.:	5810
Name of Contractor:	TELEDYNE, INC.
Contract No.:	F 33657-67-C-1313
Date of Contract:	2 March 1967
Amount of Contract:	\$ 1,736,617
Contract Expiration Date:	1 March 1968
Project Manager:	William C. Dean (703) 836-7644

P. O. Box 334, Alexandria, Virginia

AVAILABILITY

This document is subject to special export controls and each transmittal to foreign governments or foreign national may be made only with prior approval of Chief, AFTAC.

This research was supported by the Advanced Research Projects Agency, Nuclear Test Detection Office, under Project VELA-UNIFORM and accomplished under the technical direction of the Air Force Technical Applications Center under Contract F 33657-67-C-1313.

Neither the Advanced Research Projects Agency nor the Air Force Technical Applications Center will be responsible for information contained herein which may have been supplied by other organizations or contractors, and this document is subject to later revision as may be necessary.

TABLE OF CONTENTS

	Page No.
ABSTRACT	
1. INTRODUCTION	1
2. DESCRIPTION OF DATA	5
3. RESULTS	6
Multiple Coherence	6
Power Spectra	7
Stationarity Tests	7
4. CONCLUSIONS	9
FIGURES	
APPENDIX 1	1-1
Multiple Coherence Functions	
APPENDIX 2	2-1
Theoretical Development of The Stationarity Relations	
A. Noise Reduction Within The Fitting Interval	2-1
B. Noise Reduction Outside The Fitting Interval	2-3
REFERENCES	

ABSTRACT

Multiple coherence gives a quantitative measure versus frequency of how well a linear combination of n input channels can match the $(n + 1)$ st channel in a seismic array. If the inputs can match the output exactly, then the multiple coherence is unity and only n channels for short period noise fields at UBSO and TFSO.

The multiple coherence of the noise at UBSO and TFSO short period, vertical component arrays is high (greater than 0.9) over the microseismic frequency band.

The decay of the multiple coherence of the noise with increasing frequency is faster at TFSO than at UBSO and faster at UBSO than at LASA.

1. INTRODUCTION

Most basic data processing techniques for signal enhancement or identification depend upon the structure of the noise within the seismic array. If some of the coherent noise is due to site characteristics such as consistently coherent noises from particular direction, then techniques using multiple coherence will help to isolate these consistent linear relations. Many optimum filters for estimating the signal take account of these linear relations implicitly by weighting with the inverse of the spectral noise matrix. However, one cannot tell whether the coherent noise involved is due to noise generating events which cannot be predicted or controlled. Thus, the filters must be recalculated over a period of noise recording immediately prior to the arrival of each single signal. Part of the coherent noise generated within the array may be due to various causal factors for a particular array. If so, we can learn something about these factors by examining the linear relations between the various array elements. A potential benefit here is that a consistent linear model relating the different sub-elements would eliminate the need for computing a different set of filter coefficients for each event.

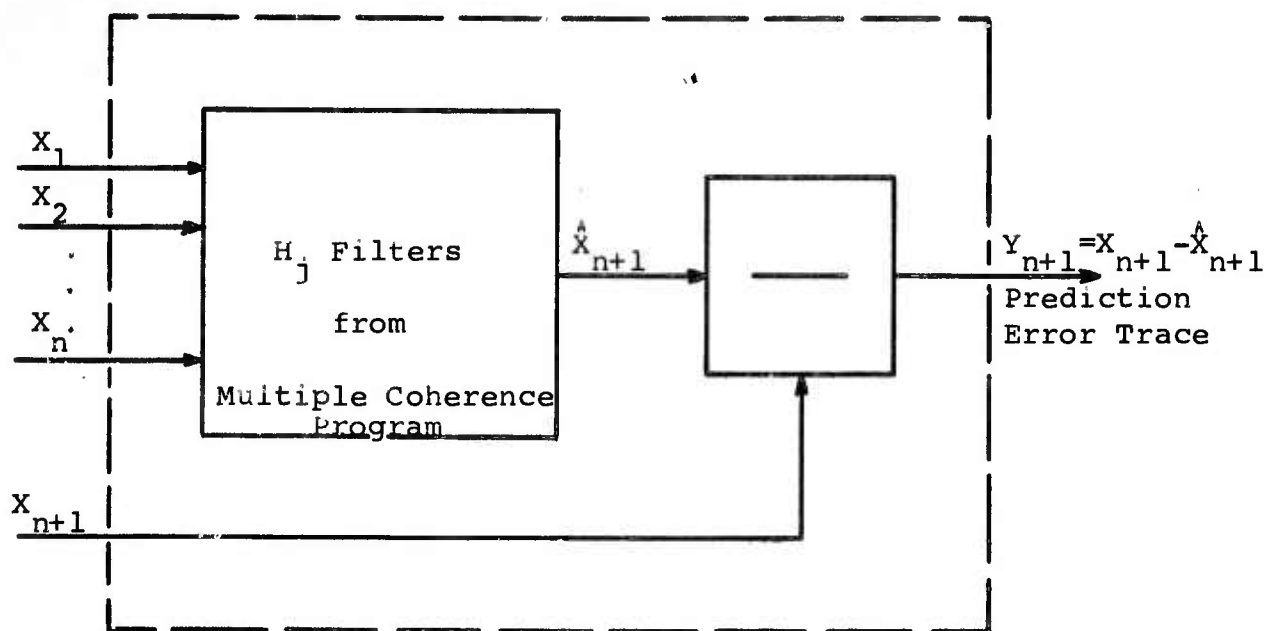
The multiple coherence function can indicate how many seismometer outputs in an array are necessary to properly determine the seismic noise field. If there are n independent seismic noise components, then the multiple coherence function would be unity when $(n + 1)$ st seismometers are placed in an array to measure seismic noise records. If part of the background is composed of incoherent noise, then the multiple coherence function would indicate the percentage of coherent noise present and the number

of seismometers necessary to define this coherent noise. The filter relations determined by the multiple coherence computations can then be used in array summation to bring the noise into destructive interference*.

This analysis does not guarantee that such optimum processing is possible. For example, if the noise and signal propagation characteristics across the array are identical, no velocity filtering scheme can be expected to separate the two even though the multiple coherence might be unity.

The multiple coherence function is the frequency domain equivalent of the prediction error filter in time. If n input seismic traces predict the $(n + 1)$ st trace in an array completely, then the multiple coherence will be unity and a prediction error filter could be used to exactly predict this $(n + 1)$ st output. In fact, linear filter relations derived by the multiple coherence program produce an estimate of the $(n + 1)$ st trace which, when subtracted from the actual $(n + 1)$ st trace, given a prediction error trace. Thus the combination of the filter derived in the multiple coherence program and the subtraction operation produces a prediction error filter as shown in the following diagram.

*For the mathematical description of the multiple coherence computation, See Appendix 1.



Prediction Error Filter

The first objective of this study is to use the multiple coherence function to estimate the degree of predictability of the short period noise field at UBSO and TFSO. The multiple coherence from these two vertical component arrays we will compare with the similar analysis for the short period LASA arrays (See SDL Report #190, "Multiple Coherence of Short Period Noise at LASA", W.C. Dean, E.F. Chiburis, 26 June 1967).

The second objective is to determine from multiple coherences the number of independent components comprising a given noise field and the percentage of incoherent noise which cannot be cancelled by any kind of multichannel filtering.

The third objective is to determine the stationarity properties of the noise field. We accomplish this by applying the multiple coherence program to three different time samples from the same array. Then the multiple coherency filters derived from the first time sample are applied to the other two time samples. If the filters derived in the first time sample have done a good job

of predicting the noise field in all three samples, then the data are said to be stationary. On the other hand, if the filters from the first time sample do a progressively poorer job of predicting the noise in the other samples relative to the filters associated with those samples, then the noise is non-stationary to some degree. This deterioration in predictability of the multiple coherence filter can quantitatively measure the non-stationarity of the data**.

** For a theoretical discussion of the stationarity computation, See Appendix II.

2. DESCRIPTION OF DATA

We computed the multiple coherences from arrays of short period, vertical component seismometers at UBSO and TFSO. The output seismometer was the center element, seismometer Z-10 at UBSO and seismometer Z-21 at TFSO. The array diagrams appear on the figures showing the multiple coherence plots. At each observatory the first inputs added were from the outermost elements of the array. The number of input channels increases from 2 to a maximum of 9. The multiple coherence is plotted vs. frequency with the number of input channels as the parameter. Since adding one additional channel to the set of inputs may not increase but can never decrease the amount of input information about a noise field, the multiple coherence must be a monotonically increasing function with increasing number of inputs.

The samples were slightly over three minutes long. The noise examined at each array came from two samples, one recorded on August 1966 and the second in January 1967. Stationarity tests were conducted on the August samples where three successive 3-minute samples were recorded.

3. RESULTS

Multiple Coherence

Figure 1 shows the multiple coherences versus frequency for two time samples separated by three minutes and recorded at UBSO on 25 August 1966. A diagram of the array elements chosen is shown at the center of the figure. The ordering of the inputs is from the outefmost to the closest and is listed in the figure. The multiple coherences are computed every .1 cps over a range from .1 to 2.6 cps. The number of points in each sample is 2000. The number of lags computed in the correlation function is 50. The data sampling rate is 10 points per second.

A similar plot of multiple coherence versus frequency for a sample recorded on 7 January 1967 at UBSO is shown in Figure 2. The number of lags used in the correlation is sufficient to detect any propagating noise component with a velocity greater than .5 km per second. Thus lack of sufficient lags cannot be a cause of low multiple coherence. The multiple coherences are high for the frequencies in the microseismic range but fall to low levels for frequencies from 1 to 2 cps. As more inputs are added the multiple coherence remains high for higher frequencies. With 9 inputs, the multiple coherence stays above .8 or .9 for all frequencies less than 1 cps. However, with this many input channels the closest inputs are only $\frac{1}{2}$ km from the output.

Figures 3 and 4 show similar effects at TFSO. Here the multiple coherence falls to a low value at frequencies well below those at UBSO. However, one must again note that the dimensions at the TFSO array are greater than those at UBSO. When we compare

the multiple coherences at the two arrays with the minimum seismometer separations from the output trace at UBSO held about equal to those at TFSO, we still find that the multiple coherence at TFSO decays faster with increasing frequency than that at UBSO.

In comparing the multiple coherences at UBSO and TFSO with those within a subarray at LASA we find that the multiple coherences at all three arrays are large for the microseismic frequencies and decay with increasing frequency. The multiple coherences at LASA remain high, greater than .8 or .9, out to frequencies higher than either UBSO and TFSO. The closest seismometers at LASA have a spacing similar to those found at UBSO. Thus we see that the noise field at LASA is more coherent with 8 or 9 inputs than that at UBSO or TFSO in the signal band.

Power Spectra

Spectra for two of the multiple coherence examples on Figures 1-4 are shown on Figures 5 and 6. The figures show the output power spectra and the range of input spectra for 8 inputs on Figure 5 and for 5 inputs on Figure 6. These two spectra are representative of all spectra for the multiple coherence examples computed in this report.

Stationarity Tests

The multiple coherence program derives a set of n filters for the n input seismograms which together provide the best linear estimate for the $(n + 1)$ st seismic trace. The difference between the observed $(n + 1)$ st trace and the best estimate is the error trace. If the multiple coherence is unity, the prediction is perfect and the error trace will be zero. If we form the ratio

of the error spectra over the observed spectra, we can get a measure of the reduction in noise power possible from the theoretical optimum filters. Thus the db improvement as a function of frequency can be expressed as

$$\text{db} = 10 \log (\text{error/observed}).$$

The prediction error filters will do the best job in eliminating the noise background when they are applied to the noise sample from which they are derived. However, if the noise is stationary, the same filter could be expected to do nearly as well when applied to later time samples from the same array. Figure 7 shows the expected noise reduction in db when the prediction error filters that were derived from the first time sample are applied to the first time sample. In addition these same filters are applied to the second and third time samples. The three 3-minute time samples are adjacent to each other. Figure 7 shows that reduction of the noise background from a prediction error filter is expected to be over 30 db in the fitting interval for the microseismic frequencies and within 2-3 db of this level on adjacent time samples. At higher frequencies the expected noise reduction in the fitting interval falls steadily until only 1 to 2 db reduction is expected for frequencies higher than 1.5 cps. In the adjacent time samples the expected noise reduction is within 1-2 db less over all frequencies.

Figures 8, 9, and 10 show similar plots over expected noise reduction for 3 adjacent time samples at TFSO. On Figure 8, sample 1 is the fitting interval. On Figure 9, sample 2; and on Figure 10, sample 3 is the fitting interval. The curves at TFSO show results similar to that at UBSO. The main differences are that the noise reduction in the microseismic band at TFSO is a bit lower than that expected at UBSO and the expected noise reduction falls to essentially zero db at 1.2 cps instead of 1.5 cps at UBSO.

4. CONCLUSIONS

1. The multiple coherence of the noise at UBSO and TFSO short period, vertical component arrays is high (greater than 0.9) over the microseismic frequency.

2. The decay of the multiple coherence of the noise with increasing frequency is faster at TFSO than at UBSO and faster at UBSO than at LASA subarrays.

3. The noise has a low multiple coherence (less than .4) with up to 9 inputs at UBSO and TFSO for frequencies greater than 1.5 cps. Thus the noise is largely incoherent over the upper part of the signal band at UBSO and TFSO.

4. The noise at UBSO and TFSO over adjacent time samples is stationary only over the microseismic frequency band.

FIGURES

1. Multiple Coherences vs. Frequency with 1-7 Inputs for two noise samples recorded at UBSO, August 1966.
2. Multiple Coherence vs. Frequency with 2-8 Inputs for two noise samples recorded at UBSO, January 1967.
3. Multiple Coherences vs. Frequency with 2-5 Inputs for two noise samples recorded at TFSO, August 1966.
4. Multiple Coherences vs. Frequency with 2-9 Inputs for two noise samples recorded at TFSO, January 1967.
5. Spectra of short period vertical components recorded at UBSO, August 1966.
6. Spectra of short period vertical components recorded at TFSO, August 1966.
7. Expected noise reduction from a prediction error filter applied to the fitting interval and two adjacent time intervals for noise recorded at UBSO in August, 1966.
8. Expected noise reduction from a prediction error filter applied to the fitting interval and two adjacent time intervals for noise recorded at TFSO in August 1966. The fitting interval is the first interval.
9. Expected noise reduction from a prediction error filter applied to the fitting interval and two adjacent time intervals for noise recorded at TFSO in August 1966. The fitting interval is the second interval.
10. Expected noise reduction from a prediction error filter applied to the fitting interval and two adjacent time intervals for the noise recorded at TFSO in August 1966. The fitting interval is the third interval.

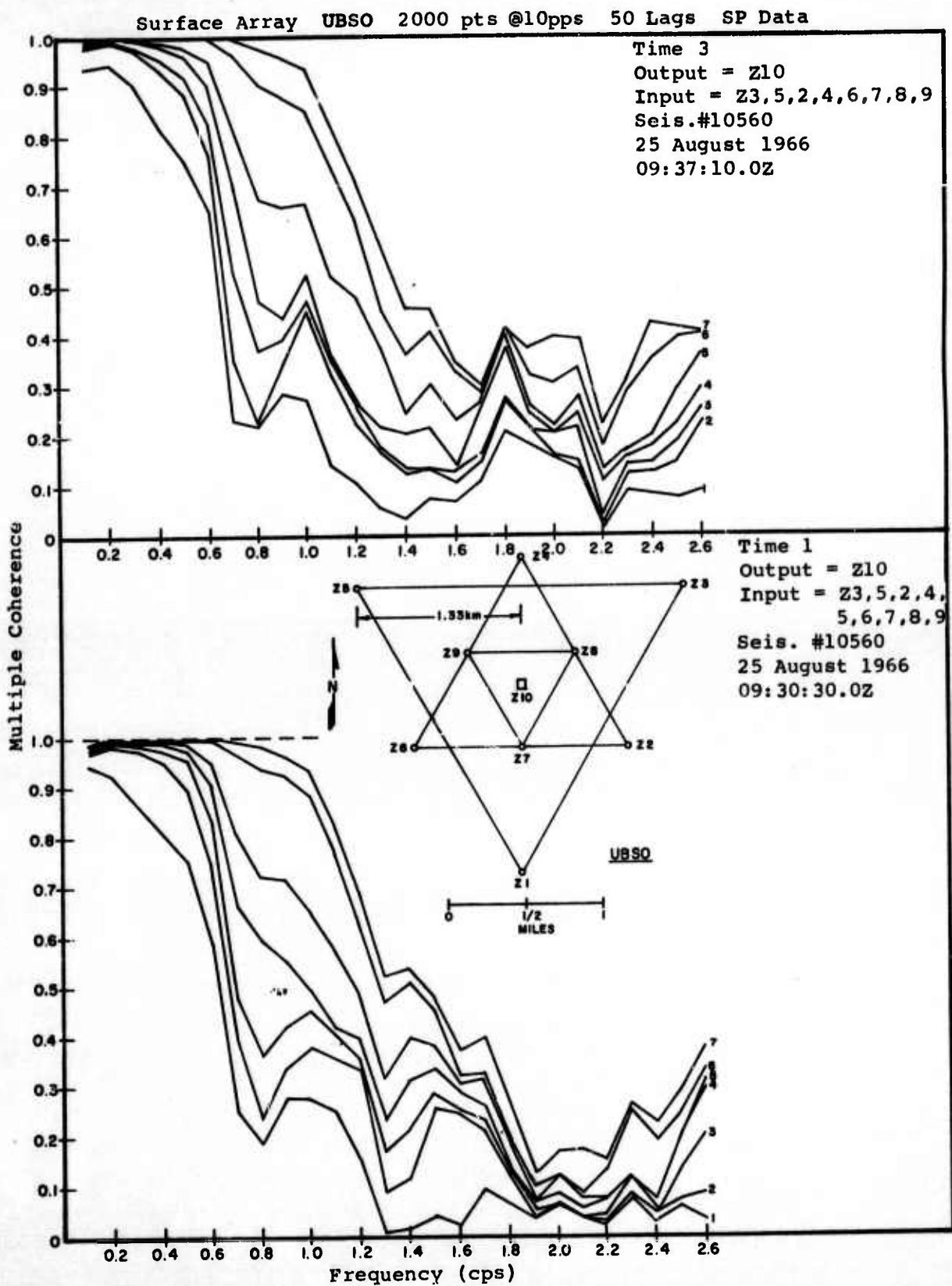


Figure 1. Multiple Coherences vs. Frequency with 1-7 Inputs for two noise samples recorded at UBSO, August 1966.

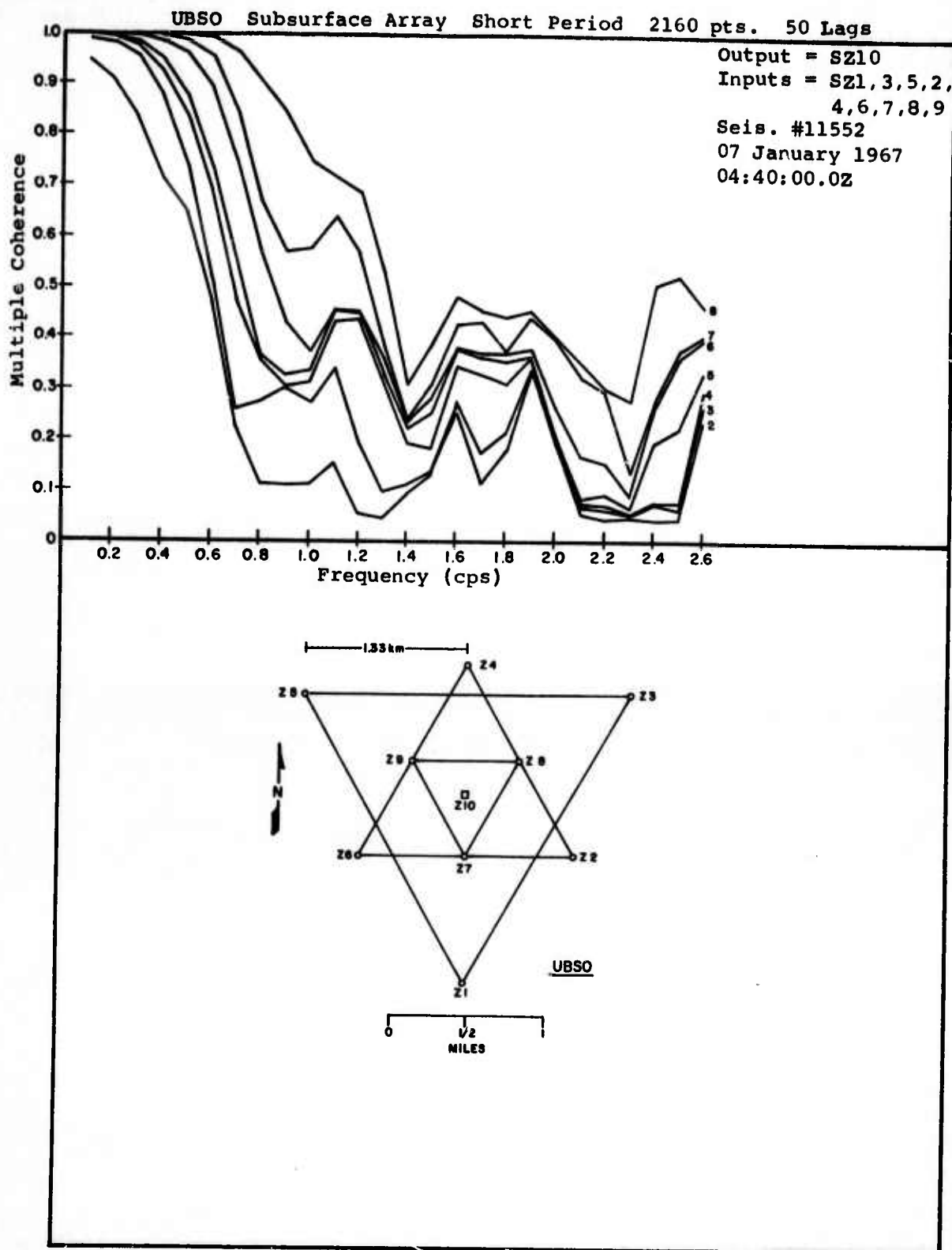


Figure 2 Multiple Coherence vs. Frequency with 2-8 Inputs for two noise samples recorded at UBSO, January 1967.

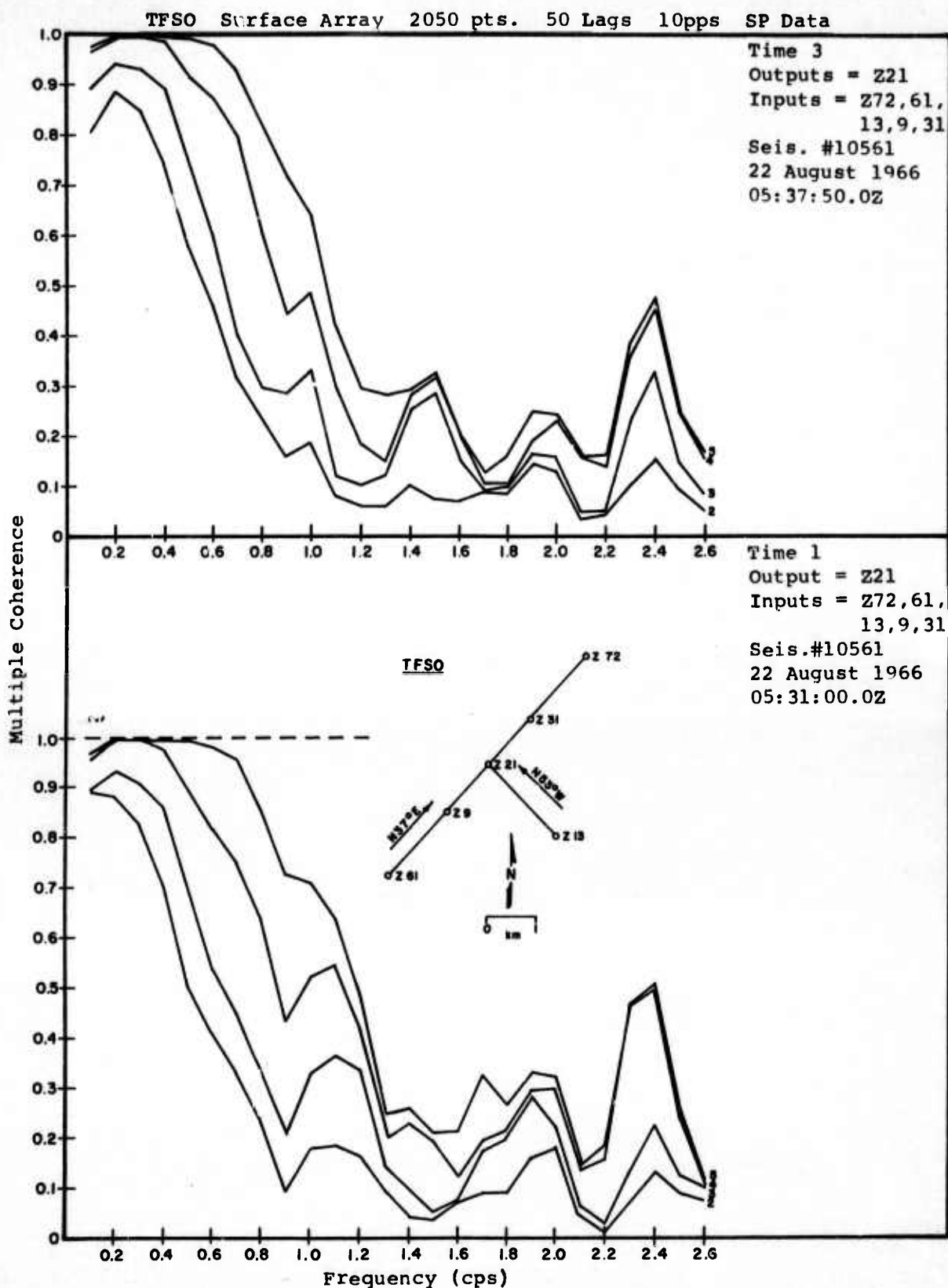


Figure 3. Multiple Coherences vs. Frequency with 2-5 Inputs for two noise samples recorded at TFSO, August 1966.

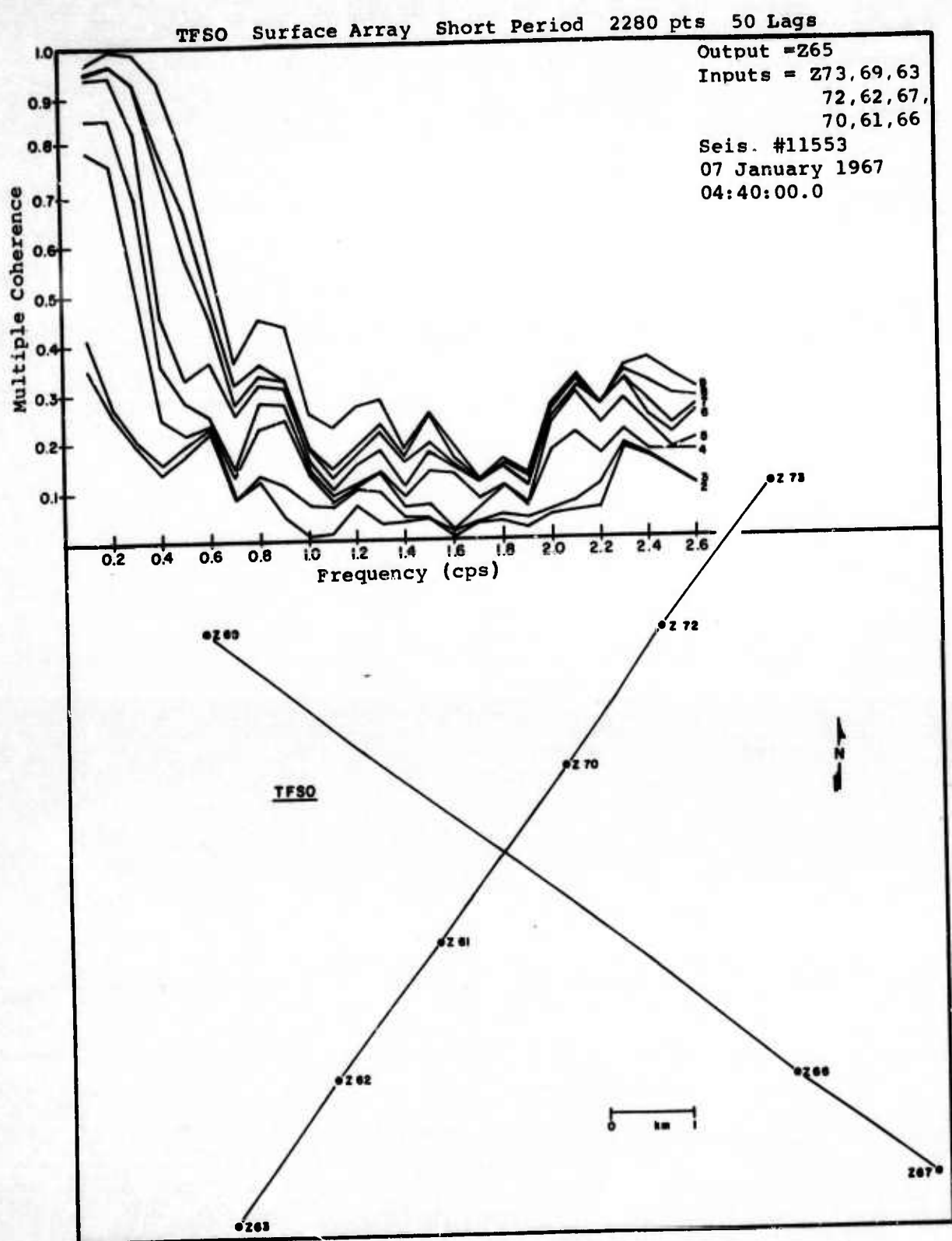


Figure 4. Multiple Coherences vs. Frequency with 2-9 Inputs for two noise samples recorded at TFSO, January 1967.

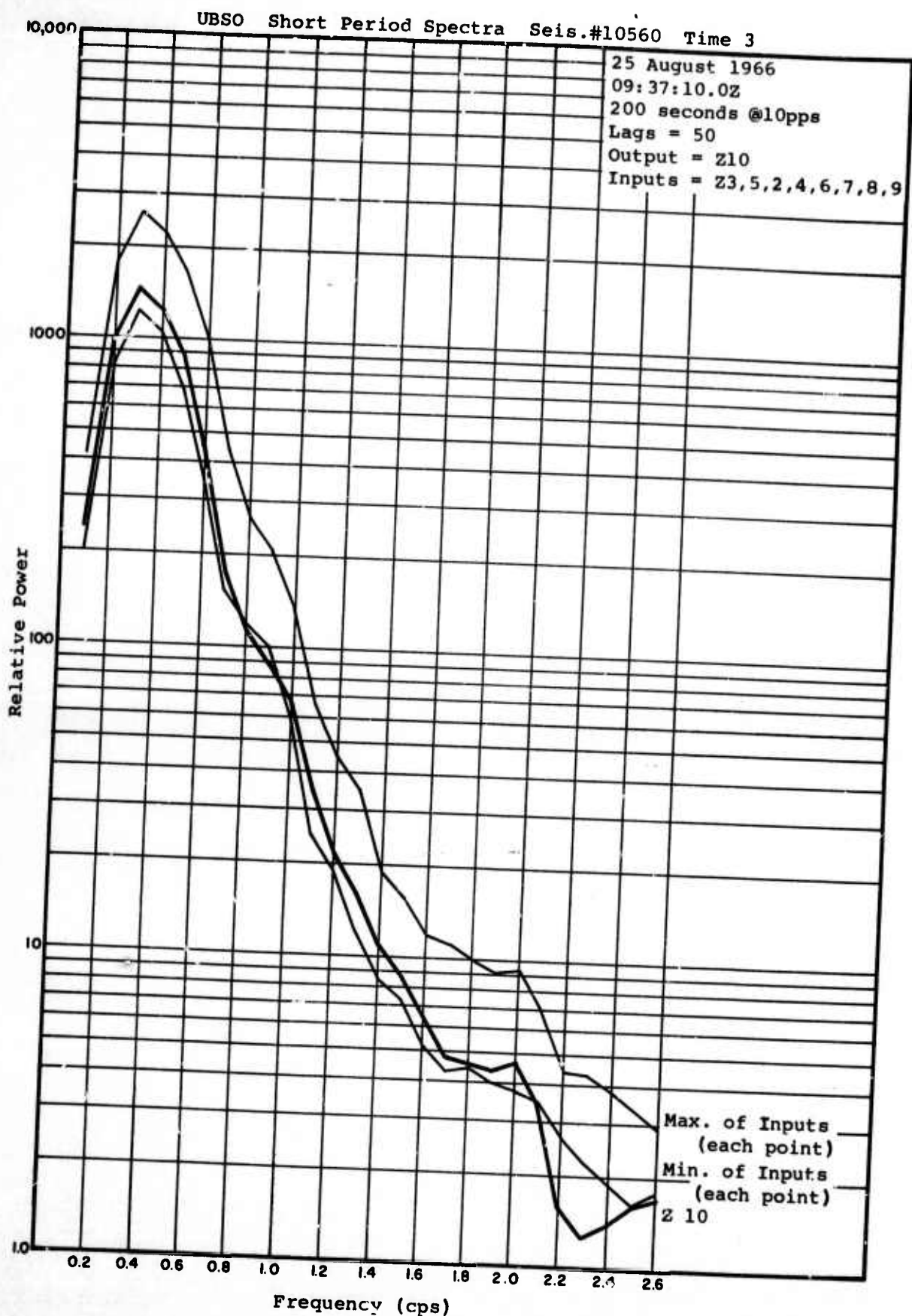


Figure 5. Spectra of short period vertical components recorded at UBSO, August 1966.

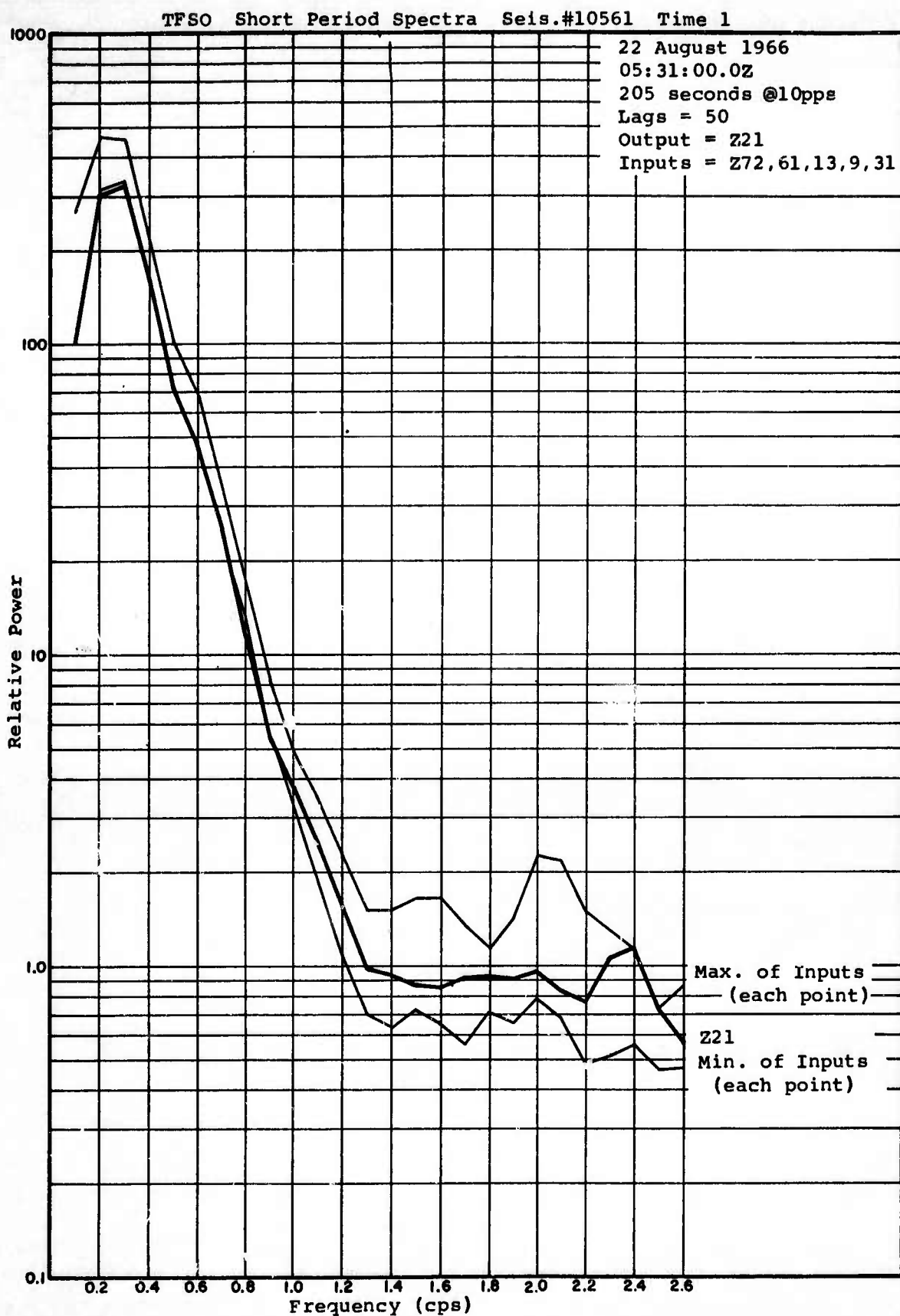


Figure 6. Spectra of short period vertical components recorded at TFSO, August 1966.

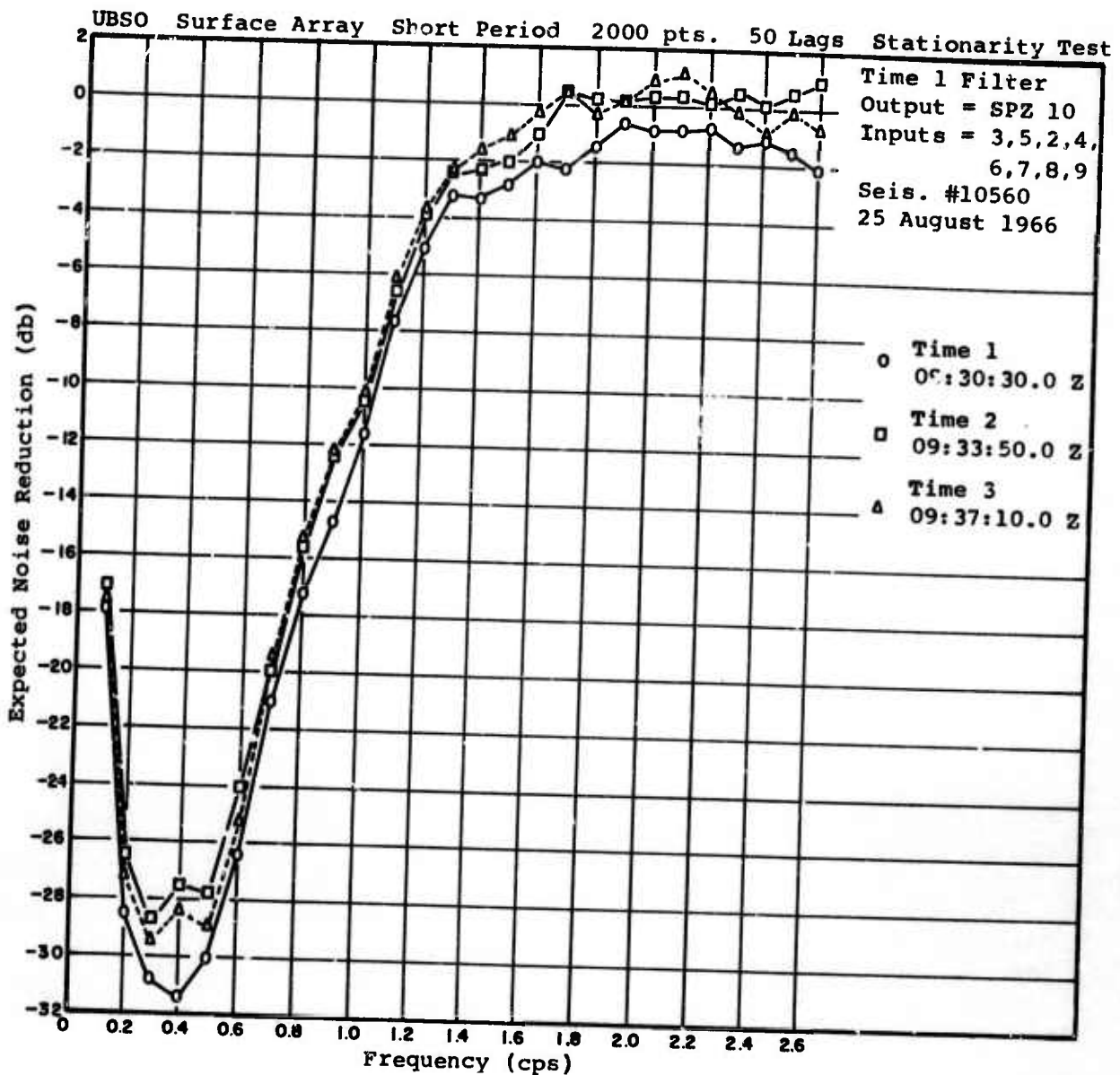


Figure 7. Expected noise reduction from a prediction error filter applied to the fitting interval and two adjacent time intervals for noise recorded at UBSO in August, 1966.

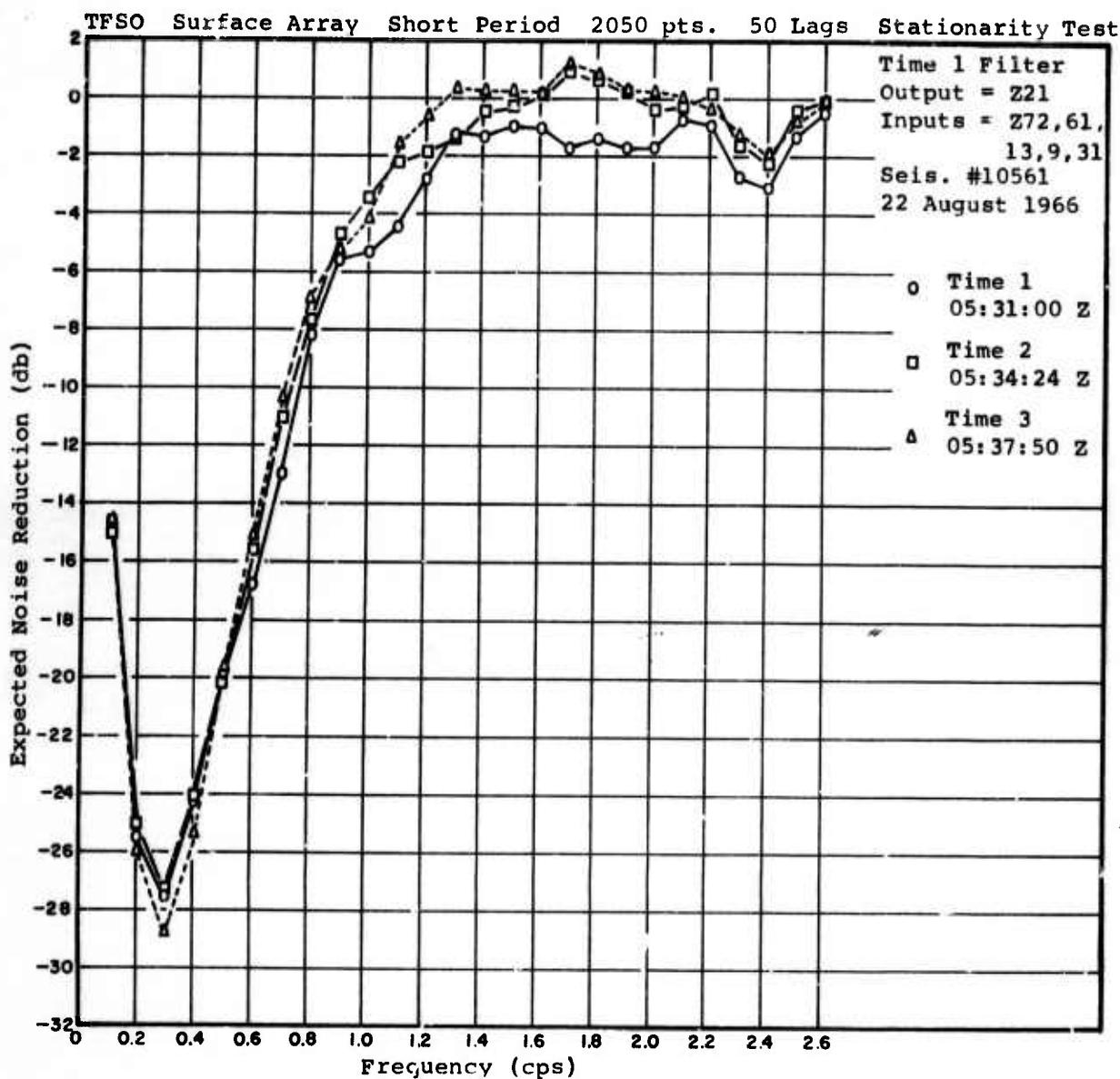


Figure 8. Expected noise reduction from a prediction error filter applied to the fitting interval and two adjacent time intervals for noise recorded at TFSO in August 1966. The fitting interval is the first interval.

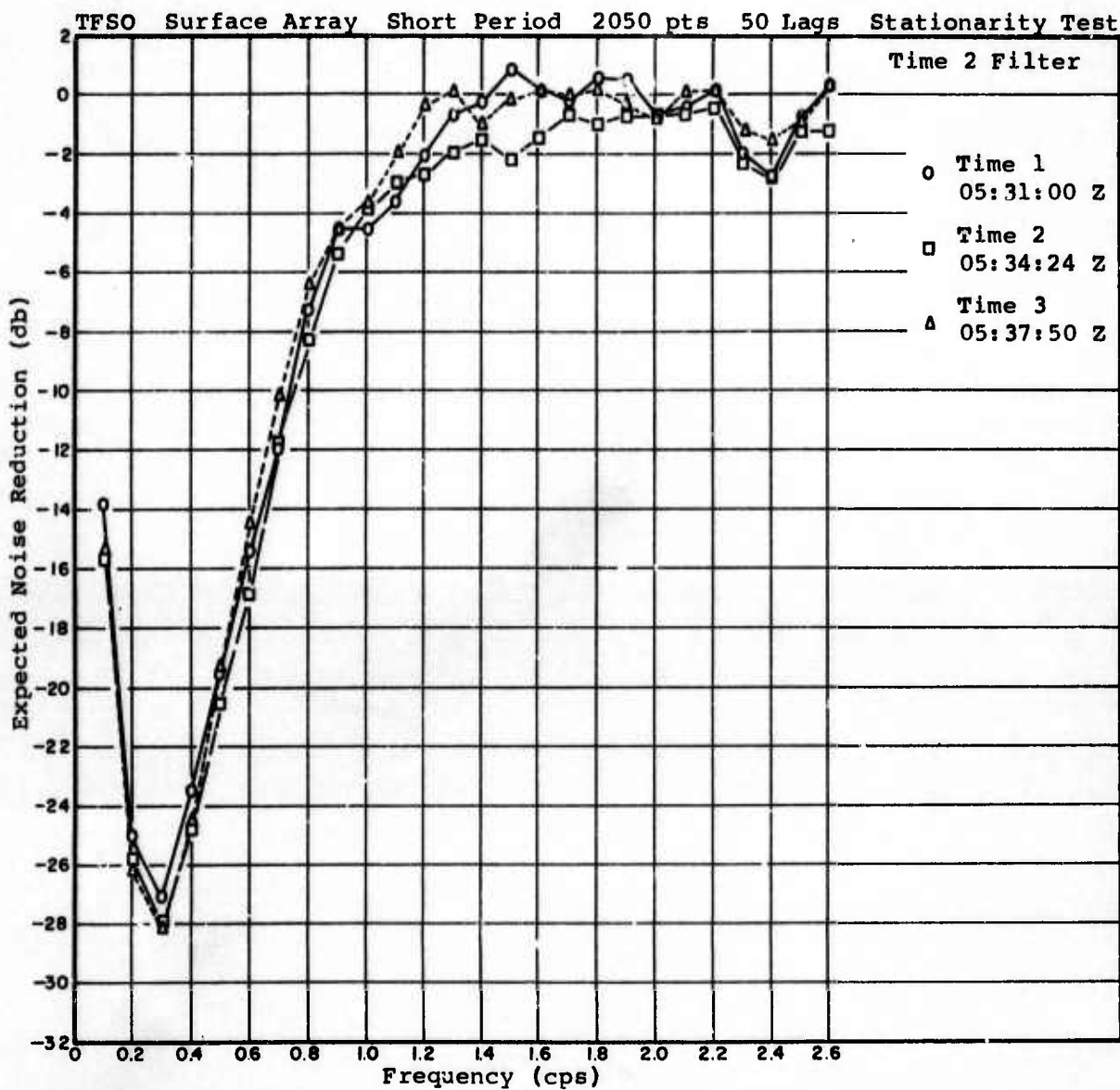


Figure 9. Expected noise reduction from a prediction error filter applied to the fitting interval and two adjacent time intervals for noise recorded at TFSO in August 1966. The fitting interval is the second interval.

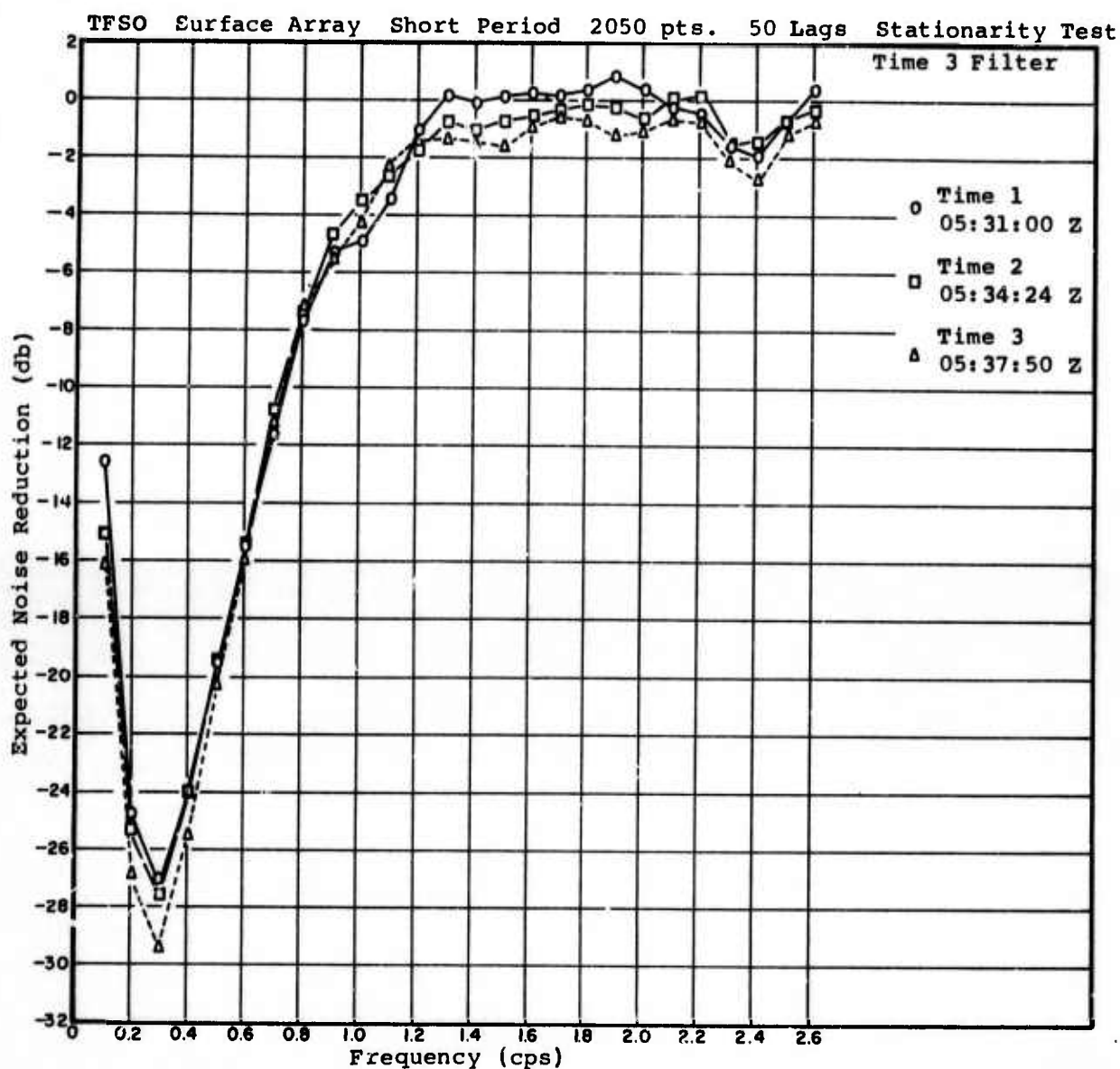


Figure 10. Expected noise reduction from a prediction error filter applied to the fitting interval and two adjacent time intervals for the noise recorded at TFSO in August 1966. The fitting interval is the third interval.

APPENDIX I

*Multiple Coherence Functions

Consider a collection of q clearly defined inputs $x_i(t)$; $i = 1, 2, \dots, q$, and one output $y(t)$, as pictured in Figure 5.12.

Let $G_i(f) = G_{ii}(f)$ be the

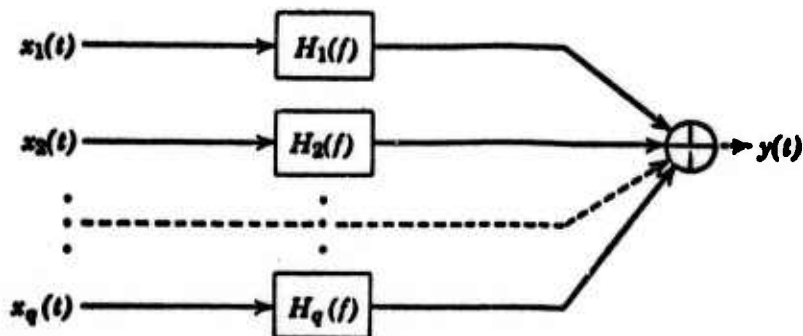


Figure 5.12 Multiple-input linear system.

power spectral density function for $x_i(t)$, and $G_{ij}(f)$ be the cross-spectral density function between $x_i(t)$ and $x_j(t)$. Define the $N \times N$ spectral matrix by

$$G_{ss}(f) = \begin{bmatrix} G_{11}(f) & G_{12}(f) & \cdots & G_{1q}(f) \\ G_{21}(f) & G_{22}(f) & & G_{2q}(f) \\ \vdots & \vdots & & \vdots \\ G_{q1}(f) & G_{q2}(f) & & G_{qq}(f) \end{bmatrix} \quad (1)$$

*This explanation of multiple coherence functions was taken from "Measurement and Analysis of Random Data", Bendat, J. S., and Piersol, A. G., John Wiley and Sons, 1966. For more detailed theoretical developments and discussions of multiple, partial and marginal coherence functions, see this text.

The ordinary coherence function between $x_i(f)$ and $x_j(f)$ is defined by

$$\gamma_{ij}^2(f) = \frac{|G_{ij}(f)|^2}{G_i(f) G_j(f)} \quad (2)$$

The multiple coherence function between $x_i(f)$ and all other inputs $x_1(f), x_2(f), \dots$, excluding $x_i(f)$, is defined by

$$\gamma_{i..}^2(f) = 1 - [G_i(f) G'(f)]^{-1} \quad (3)$$

where $G^i(g)$ denotes the i th diagonal element of the inverse matrix $G_{xx}^{-1}(f)$ associated with Eq. (1). The ordinary and multiple coherence functions are both real-valued quantities which are bounded by zero and unity. That is,

$$\begin{aligned} 0 \leq \gamma_{ij}^2(f) \leq 1 \\ 0 \leq \gamma_{i..}^2(f) \leq 1 \end{aligned} \quad (4)$$

The multiple coherence function is a measure of the linear relationship between the time history at one point, and the time histories at the collection of other points. That is, the multiple coherence function indicates whether or not the data at all of the other points linearly produce the results at a given point.

APPENDIX 2

Theoretical Development of The Stationarity Relations

A. Noise Reduction Within The Fitting Interval

A number of useful statistical measures such as ordinary and multiple coherence can be used as tools to indicate the amount of noise reduction feasible in a multiply coherent array. The basic linear model which determines the db reduction possible in the noise field by multiple coherence filtering relates a reference element (trace) $y(t)$ of an array to the other elements, say $x_1(t)$, $x_2(t)$, ..., $x_p(t)$ in the array through the linear model

$$y(t) = \sum_{k=1}^P \int_{-\infty}^{\infty} h_k(\alpha) x_k(t-\alpha) d\alpha \quad (1)$$

Generally we determine $h_k(t)$ as the time invariant linear filter that makes the mean square error between $y(t)$ and its predicted value a minimum, i. e.

$$E \left| y(t) - \sum_{k=1}^P \int_{-\infty}^{\infty} h_k(\alpha) x_k(t-\alpha) d\alpha \right|^2 = \min \quad (2)$$

which, by the usual orthogonality principle (see Papoulis 1), yields the condition

$$E y(t) x_l(t+\tau) = \sum_{k=1}^P \int_{-\infty}^{\infty} h_k(\alpha) E x_k(t-\alpha) x_l(t+\tau) d\alpha$$

$$l = 1, 2, \dots, p, -\infty < \tau < \infty \quad (3)$$

$$\text{or} \\ R_{yx_l}(\tau) = \sum_{k=1}^P \int h_k(\alpha) R_{x_k x_l}(\tau + \alpha) d\alpha \quad (4)$$

which by taking Fourier transforms implies that

$$S_{yx_l}(\omega) = \sum_{k=1}^P H_k^*(\omega) S_{x_k x_l}(\omega) \quad (5)$$

Now, the mean square error can be written

$$\begin{aligned} E|y(t) - \sum_{k=1}^P \int h_k(\alpha) x_k(t-\alpha) d\alpha|^2 &= E \left(y(t) - \sum_{k=1}^P \int_{-\infty}^{\infty} h_k(\alpha) x_k(t-\alpha) d\alpha \right) y(t) \\ &= R_{yy}(0) - \sum_{k=1}^P \int h_k(\alpha) R_{x_k y}(\alpha) d\alpha \\ &= \int_{-\infty}^{\infty} \left[S_{yy}(\omega) - \sum_{k=1}^P H_k^*(\omega) S_{x_k y}(\omega) \right] \frac{d\omega}{2\pi} \\ &= \int_{-\infty}^{\infty} \left(S_{yy} - \frac{S_{yx}}{S_{xx}} S_{xx}^{-1} S_{xy} \right) (\omega) \frac{d\omega}{2\pi} \\ &= \int_{-\infty}^{\infty} \left(1 - \alpha^2(\omega) \right) S_{yy}(\omega) \frac{d\omega}{2\pi} \end{aligned} \quad (6)$$

where $\alpha^2(\omega)$ is the multiple coherence and $(1 - \alpha^2(\omega))$ measures the reduction in power possible at the frequency ω . With $\alpha^2(\omega) = 1$ the mean square error is zero and with $\alpha^2(\omega) = 0$ the mean square error is just

$$\int_{-\infty}^{\infty} S_{yy}(\omega) \frac{d\omega}{2\pi} = R_{yy}(0) = E|y(t)|^2 \quad (7)$$

which is the original power in the process $y(t)$. Now the quantity $(1-\alpha^2(\omega)) S_{yy}(\omega)$ represents the residual power at each frequency after the best linear estimate of the form (1) has been subtracted out. Hence the db reduction in power at each frequency is just the ratio of the output power of the residual (see equation (2)) to the input power in $y(t)$ or

$$I_H(\omega) = 10 \log \frac{S_{ee}(\omega)}{S_{yy}(\omega)} = 10 \log (1 - \alpha^2(\omega)) \quad (8)$$

where $\alpha^2(\omega)$ is the multiple coherence and $S_{ee}(\omega)$ is the power spectrum of the error process

$$e(t) = y(t) - \sum_{k=1}^P \int_{-\infty}^{\infty} h_k(\alpha) x_k(t - \alpha) d\alpha \quad (9)$$

B. Noise Reduction Outside The Fitting Interval

We would also like to determine the noise reduction in db which would result from using a set of filters $g_k(t)$, $k=1, \dots, p$ which have been derived either from another fitting interval or from theoretical considerations. To accomplish this let $h_k(t)$ be the optimal filters for the time under investigation and let $g_k(t)$ be any other set of filters whose mean square error is to be compared with $h_k(t)$. The mean square error of the g filters can be written using the orthogonality principle as

$$E \left| y(t) - \sum_{k=1}^P \int_{-\infty}^{\infty} g_k(\alpha) x_k(t - \alpha) d\alpha \right|^2$$

$$\begin{aligned}
& E|y(t) - \sum_{k=1}^P \int_{-\infty}^{\infty} h_k(\alpha) x_k(t-\alpha) d\alpha + \sum_{k=1}^P \int_{-\infty}^{\infty} (h_k(\alpha) - g_k(\alpha)) x_k(t-\alpha) d\alpha|^2 \\
& = E|y(t) - \sum_{k=1}^P \int_{-\infty}^{\infty} h_k(\alpha) x_k(t-\alpha) d\alpha|^2 + E| \sum_{k=1}^P \int_{-\infty}^{\infty} (h_k(\alpha) - g_k(\alpha)) x_k(t-\alpha) d\alpha|^2 \\
& = \int_{-\infty}^{\infty} (1 - \alpha^2(\omega)) S_{YY}(\omega) \frac{d\omega}{2\pi} + \int_{-\infty}^{\infty} (\underline{H} - \underline{G})^* S_{XX} (\underline{H} - \underline{G}) (\omega) \frac{d\omega}{2\pi} \\
& = \int_{-\infty}^{\infty} \left[(1 - \alpha^2(\omega)) + \frac{(\underline{H} - \underline{G})^* S_{XX} (\underline{H} - \underline{G}) (\omega)}{S_{YY}(\omega)} \right] S_{YY}(\omega) \frac{d\omega}{2\pi} \quad (10)
\end{aligned}$$

Hence, if we call the new error $e'(t)$ we have

$$e'(t) = y(t) - \sum_{k=1}^P \int_{-\infty}^{\infty} g_k(\alpha) x_k(t-\alpha) d\alpha$$

with power spectrum $S_{e'e'}(\omega)$, the new value for the improvement in the $S_k(t)$ filters would be

$$I_G(\omega) = 10 \log \frac{S_{e'e'}(\omega)}{S_{YY}(\omega)} = 10 \log_S \left(1 - \alpha^2(\omega) + \frac{(\underline{H} - \underline{G})^* S_{XX} (\underline{H} - \underline{G}) (\omega)}{S_{YY}(\omega)} \right) \quad (12)$$

Equation (12) shows that the improvement in the $g_k(t)$ filters is expressed in terms of the improvement in the $h_k(t)$ filters and a correction term which is zero when $\underline{H} = \underline{G}$.

The improvement values $I_H(\omega)$ and $I_G(\omega)$ in equations (8) and (12) are those shown in the main body of the report.

Reference

1. Papoulis, A., Probability, Random Variables, and Stochastic Processes, McGraw Hill, 1965.

Unclassified
Security Classification

DOCUMENT CONTROL DATA - R&D		
(Security classification of title, body of abstract and indexing annotation must be entered when the overall report is classified)		
1. ORIGINATING ACTIVITY (Corporate author) TELEDYNE, INC. ALEXANDRIA, VIRGINIA		2a. REPORT SECURITY CLASSIFICATION Unclassified 2b. GROUP --
3. REPORT TITLE MULTIPLE COHERENCE OF SHORT PERIOD NOISE AT UBSO AND TFSO.		
4. DESCRIPTIVE NOTES (Type of report and inclusive dates) Scientific		
5. AUTHOR(S) (Last name, first name, initial) Chiburis, E. F. and Dean, W. C.		
6. REPORT DATE June 30, 1967	7a. TOTAL NO. OF PAGES 29	7b. NO. OF REFS 1
8a. CONTRACT OR GRANT NO. F 33657-67-C-1313 b. PROJECT NO. VELA T/6702 c. ARPA Order No. 624 d. ARPA Program Code No. 5810	9a. ORIGINATOR'S REPORT NUMBER(S) 192 9b. OTHER REPORT NO(S) (Any other numbers that may be assigned this report)	
10. AVAILABILITY/LIMITATION NOTES This document is subject to special export controls and each transmittal to foreign governments or foreign national may be made only with prior approval of Chief, AFTAC.		
11. SUPPLEMENTARY NOTES ----	12. SPONSORING MILITARY ACTIVITY ADVANCED RESEARCH PROJECTS AGENCY NUCLEAR TEST DETECTION OFFICE WASHINGTON, D. C.	
13. ABSTRACT Multiple coherence gives a quantitative measure versus frequency of how well a linear combination of n input channels can match the (n + 1)st channel in a seismic array. If the inputs can match the output exactly, then the multiple coherence is unity and only n channels for short period noise fields at UBSO and TFSO. The multiple coherence of the noise at UBSO and TFSO short period, vertical component arrays is high (greater than 0.9) over the microseismic frequency band. The decay of the multiple coherence of the noise with increasing frequency is faster at TFSO than at UBSO and faster at UBSO than at LASA.		

DD FORM 1 JAN 64 1473

Unclassified
Security Classification